NEURAL REGENERATION RESEARCH
June 2014, Volume 9, Issue 12
www.nrronline.org

Diffuse axonal injury after traumatic cerebral microbleeds: an evaluation of imaging techniques

Jun Liu[1, 2, 3], **Zhifeng Kou**[2], **Yongquan Tian**[3]

1 Department of Radiology, Second Xiangya Hospital, Central South University, Changsha, Hunan Province, China
2 Department of Biomedical Engineering and Radiology, School of Medicine, Wayne State University, 3990 John R St, Detroit, MI, USA
3 School of Public Administration, Central South University, Changsha, Hunan Province, China

Corresponding author:
Yongquan Tian, M.D, School of Public Administration, Central South University, Changsha 410083, Hunan Province, China, tianyq@csu.edu.cn.

doi:*10.4103/1673-5374.135330*
http:*//www.nrronline.org/*

Accepted: *2014-04-01*

Abstract

Previous neuropathological studies regarding traumatic brain injury have primarily focused on changes in large structures, for example, the clinical prognosis after cerebral contusion, intracerebral hematoma, and epidural and subdural hematoma. In fact, many smaller injuries can also lead to severe neurological disorders. For example, cerebral microbleeds result in the dysfunction of adjacent neurons and the disassociation between cortex and subcortical structures. These tiny changes cannot be adequately visualized on CT or conventional MRI. In contrast, gradient echo sequence-based susceptibility-weighted imaging is very sensitive to blood metabolites and microbleeds, and can be used to evaluate traumatic cerebral microbleeds with high sensitivity and accuracy. Cerebral microbleed can be considered as an important imaging marker for diffuse axonal injury with potential relevance for prognosis. For this reason, based on experimental and clinical studies, this study reviews the role of imaging data showing traumatic cerebral microbleeds in the evaluation of cerebral neuronal injury and neurofunctional loss.

Key Words: *nerve regeneration; neuroimaging; traumatic brain injury; cerebral microbleeds; diffuse axonal injury; gradient-recalled-echo; susceptibility weighted imaging; review; neural regeneration*

Funding: *This study was supported by grants from the State-Funded Construction Projects Key Clinical Specialist (2013-2015) and the Hunan Provincial Science and Technology Department, No. 2009FJ3092.*

Liu J, Kou ZF, Tian YQ. Diffuse axonal injury after traumatic cerebral microbleeds: an evaluation of imaging techniques. Neural Regen Res. 2014;9(12):1222-1230.

Introduction

Worldwide annual incidence of traumatic brain injury (TBI), caused by falls, motor vehicle accidents, physical assaults, and sports injuries totals approximately 7 million people per year (Song et al., 2013). Data from the most extensive report to date (using a multistate population-based TBI surveillance system) indicates the importance of TBI as a public health problem (Shimizu et al., 2013). In the United States alone, about 1.5 million people suffer TBI per year (Yin et al., 2013).

An estimated 475,000 cases of TBI occur among children below the age of 15, and it is the leading cause of death and disability in young individuals who are in the most productive period of their lives (Xiao et al., 2013a). It has therefore been referred to as "a silent epidemic" (Wang et al., 2013b). The number of Americans living with long-term disability because of TBI is as high as 5.3 million. According to a CDC report in 2000, TBI is imposing an ever growing economic burden on the US, with an annual loss amounting to $60 billion per year (Finkelstein, et al., 2006). Thus, TBI is a burning public health problem with a direct bearing on the US economy (Xiao et al., 2013b).

Overall interest in cerebral microbleeds (CMBs) has been growing rapidly in the recent years. Significantly different from larger hemorrhages, CMBs are defined as foci with increased susceptibility-weighted imaging (SWI) signals that are not consistent with bones, vessels, or MRI artifacts. An ovoid or round lesion, with low MRI signal and a diameter between 2 and 10 mm, and which is clearly not a blood vessel is considered to be a microbleed (Glenski et al., 1984; Mori et al., 2013). CMBs are visualized as small, round, and homogenous low signal lesions on gradient-recalled echo T2*-weighted images or SWI images because hemosiderin, a paramagnetic product of heme degradation, has high magnetic susceptibility and gives rise to a lesion exhibiting a homogenous signal loss. CMBs occur because of bleeding around small vessels, primarily seen in cerebral amyloid angiopathy and hypertensive vasculopathy (Zhang et al., 2013a). Red blood cells have been shown to form petechial microbleeds by passing through endothelial cells and into brain tissue *via* a phenomenon called diapedisis. Additionally, Zhong et al. (2013) showed evidence of a brief transient opening of the blood-brain barrier after traumatic injury to the brain. CMBs frequently occur at the border between cortical gray matter and white matter. The different physical properties of gray and white matter may result in differential

deformation under the same accelerative/decelerative forces, resulting in a peak strain of brain tissue at the interface between the two types of tissue. In addition, changes in venous drainage between gray and white matter may also explain the vulnerability to shear strain. Two typical patterns of bifurcation hemorrhages, which tend to be small and spherical, have been observed. Viewed in two dimensions, these hemorrhages appear to lie at the terminus of a vessel that is in the plane of the imaged slice. This can give it the appearance of a "ball atop a flagpole" in longer, straighter vessels or a "tadpole" appearance in smaller, tortuous vessels. Indeed, the "tadpole" shape micro-hemorrhage could be attributed to leaks through the blood-brain barrier where pial veins branch into venules. Consequently, leaked red blood cells accumulate at the venule-branching area. Histologically, hemorrhages may be perivascular or in the neuropil, and they are associated with diffuse axonal injury (DAI). Focal traumatic shearing or tearing of the affected blood vessels leads to bleeding into the perivascular space and/or the neural parenchyma (Zhang et al., 2014a).

CMBs should be detected and mapped reliably. Microbleeds have been shown to be involved in the pathogenesis of several neurovascular and neurodegenerative diseases. A review suggests that the occurrence of CMBs might indicate a higher risk of future intracerebral hemorrhage and may be regarded as a marker of cerebral small-vessel disease and cerebral amyloid angiopathy (Fu et al., 2013). Traumatic microbleeds (TMBs) that occur in TBI often include CMBs, and hence can be considered radiological markers of DAI with potential relevance for prognosis (Guo et al., 2013b; Kang and Zhu, 2013). There is great research interest in determining the predictive value of cerebral microbleeds (and their severity) for the incidence or recurrence of primary intracranial bleed (Sun et al., 2013b; Zhang et al., 2014b). Furthermore, several studies show that the CMB burden is both strongly and independently related to the occurrence of intracerebral bleeding in patients taking anticoagulant therapy (Xu et al., 2013; Zhu et al., 2013c). Thus, assessing the potential use of CMB burden calculation for diagnosis and prognosis of disease is important, as is assessing the subsequent usefulness of this calculated value in making decisions related to treatment. Multiple conditions can potentially cause cerebral microbleeds and iron deposition in the brain, with systemic hypertension, cerebral amyloid angiopathy, and diffuse axonal injury secondary to trauma being the most important ones (Sun et al., 2013a; Zhu et al., 2014).

Here, our purpose is to review the research progress regarding detection of cerebral microbleeds *via* imaging methods of TBI.

DAI and CMBs

DAI results from accelerative-decelerative forces associated with high-energy head trauma, which give rise to shearing forces that act at regions of the brain with different densities and compliances. Gray matter-white matter junctions and the region adjacent to the falx are the most susceptible location for this type of damage. DAI that is more common and associated with microbleeding is called hemorrhagic DAI. DAI without microbleeding or with isolated microbleeding has also been reported (Chen et al., 2013b). Intraparenchymal bleeding, including white matter microbleeding, is also a major feature of TBI. There are two manifestations of DAI. The first one is small petechial hemorrhages throughout the brain that result from the rupture of small blood vessels. The second is linear hemorrhages at subcortical white matter regions, particularly in the posterior frontal and parietal lobes (Ju et al., 2013). These small petechial hemorrhages scattered throughout the white matter, particularly in parasagittal white matter, are typically called diffuse vascular injury (DVI) (Costello et al., 2013; Zhu et al., 2013a). All cases of DVI show severe DAI and fall in a spectrum of similar pathological conditions (Chen et al., 2013a; Costello et al., 2013). Thus, appreciating the properties of DVI, as understood through microbleeding petechial hemorrhages, helps give diagnostic insight into potential DAI.

As the identification and localization of small hemorrhage foci gives useful information about the mechanism of injury and helps predict the clinical outcome, detecting intracranial hemorrhagic lesions is essential for the best treatment and management of patient with TBI.

Computed tomography (CT)

CT is a proven, time-tested method for making diagnoses, evaluating the extent and severity of intracranial hemorrhages, and for assessing progression in follow-up examinations. Short examination time and its compatibility with life-supporting devices have made it a method of choice to evaluate seriously injured patients. CT can easily detect large hemorrhagic lesions and is therefore an important screening tool for examining large hemorrhages at acute stages or other lesions that require urgent surgical intervention (Tchekmedyian et al., 2013). However, owing to its poor soft tissue resolution, it cannot detect other primary or secondary injuries, some of which can easily be identified by conventional magnetic resonance imaging (MRI). It also cannot detect small hemorrhages arising from early contusions or DAI. Thus, causes of neurological symptoms associated with DAI and other subtle pathologies cannot be determined by CT. For example, a near normal CT scan in a comatose patient after trauma is a common finding in patients with severe DAI. In addition, most mild TBI patients (mTBI), who comprise more than 90% of the total TBI patients, have negative findings on CT or conventional MRI (Warner et al., 1988a). Indeed, a study was conducted to find out which method of imaging was the most effective in predicting 6–12 month outcomes in children with TBI, as classified by the Pediatric Cerebral Performance Category Scale score. Forty children with TBI were assessed using different imaging modalities (CT, T2-weighted MRI, fluid-attenuated inversion recovery [FLAIR] MRI, and SWI), and results showed that although CT is inconsistent with detecting/predicting lesions, it is still regarded as an essential part of the acute TBI work-up performed to assess the need for neurosurgical intervention (Zen et al., 2013).

Conventional MRI

Although MRI requires a longer image acquisition time and is not compatible with instruments having magnetic components, its capacity to detect small hemorrhages is more promising compared with that of CT (Wang et al., 2014a). For instance, MRI (FLAIR) is more sensitive to subarachnoid hemorrhage (SAH) than CT, and can detect high signals in the subarachnoid space in the early stages of hemorrhage (Wu et al., 2013). MRI is increasingly being used not only to detect the primary pattern of injuries, but also the secondary effects like edema, infarction, herniation, and hemorrhage. Among MRI sequences, gradient-echo imaging is superior to spin-echo imaging for the detection of microbleeds associated with DAI (Liu et al., 2013b), particularly in hemorrhagic shearing injuries (Hou et al., 2013). While CT scans can detect the scattered hemorrhages within the brain parenchyma along with the accompanying edema that occur in traumatic brain contusions, T2-weighted MRI possesses higher sensitivity for detecting such lesions (Zhu et al., 2013f). A study revealed that MRI detects a broader spectrum of TBI than CT does. Besides primary lesions, secondary outcomes of injury such as territorial arterial infarction, pressure necrosis resulting from increased intracranial pressure, cerebral herniation, and secondary brainstem injury were also made visible by MRI in some cases. T2*-weighted images were more useful for detection of pathological lesions, whereas, T1-weighted images were more effective for anatomical delineation and classification of the lesions (Chen et al., 2013b). However, MRIs of hemorrhage are variable and depend on multiple intrinsic factors such as integrity of red blood cells, oxygenation state of hemoglobin, presence of metabolites (such as ferritin, hemosiderin, deoxyhemoglobin) of blood, as well as extrinsic factors such as field strength of the MR imaging unit, type of sequence, receiver bandwidth, and degree of T1 and T2 weighting (Shi et al., 2013a).While the presence of hemosiderin has been suggested as a biomarker of parenchymal injury (Jiang et al., 2013; Tao et al., 2013), and deposits associated with micro-hemorrhages are often too small to be detected viaspin-echo MR imaging (Gao et al., 2014), they are often detectable months after the injury using gradient-echo MRI (Cai et al., 2013; Wang et al., 2013c). A study using conventional MRI has shown that the detection of hemorrhage in DAI is a poor predictor of clinical outcome (Zhu et al., 2013j). Similarly, conventional MRI does not reliably correlate with clinical measurements such as the Glasgow Coma Scale (GCS) (Wang et al., 2013a). Initial survival is determined by acute emergency and intensive care management, and as the subacute and chronic stages of recovery progress, success becomes less predictable than during the acute stage. Conventional MRI does not appear to correlate with injury severity measured by GCS, long-term outcome measured by Glasgow Outcome Scale scores (GOS), or neuropsychological assessment. Indeed, conventional imaging adds little to non-imaging clinical measures in the prediction of long-term neurocognitive outcome.

GRE-MRI

Chronic CMBs visualized by magnetic resonance GRE imaging are thought to be an important marker of these bleeding-prone micro-angiopathies. Pathologic studies have demonstrated that GRE-visualized microbleeds usually represent hemosiderin-laden macrophages that occur adjacent to small vessels and are indicative of previous extravasation of blood (Shi et al., 2013b). Previous studies have shown that GRE-MRI detected microbleeds in 50–80% of patients with primary intracerebral hemorrhage (Tie et al., 2013; Yang et al., 2013). In the near future, microbleeds may prove to be a useful biomarker that provides an understanding of the pathophysiology of intracerebral hemorrhage, help predict the prognosis and disease progression, and guide therapeutic strategies, particularly in medically underserved populations (Zhu et al., 2013b).

A comparison study was done in 200 elderly participants using two methods of MRI imaging at 1.5T: accelerated three-dimensional (3D) T2*-weighted gradient-recalled echo (GRE) MR sequences and conventional two-dimensional (2D) T2*-weighted GRE sequences. The variables recorded with both techniques were presence, number, and location of microbleeds. Detection of CMBs was significantly higher with 3D-T2*-weighted GRE images (35.5%) than with 2D-T2*-weighted GRE images (21.0%, $P < 0.001$). Furthermore, in those brains in which microbleeds were detected by both techniques, significantly more microbleeds were detected on the 3D image sets ($P < 0.001$). For both imaging methods, proportions of participants with lesions in lobar (cortical gray and subcortical white matter), deep, or infratentorial locations showed no statistically significant difference. Thus, it can be concluded that accelerated 3D T2*-weighted GRE images detect more microbleeds than do conventional 2D T2*-weighted GRE images (Zhang et al., 2013b). Additionally, in a study comparing MRIs from 14 patients using a 1.5-3T system, the number of TMBs differed significantly depending on the system (1.5T: 239 TMBs, 3T: 470 TMBs, $P = 0.001$). However, in all patients (except one), MRI at 1.5T also clearly showed CMBs. A significant negative correlation was found between the number of TMBs and the examination time interval by using MRI after TBI, and detection of TMBs using T2*-weighted MRI at 3T was superior to that using 1.5T. However, for practical purposes, MRI at 1.5T appears to be good enough. Despite a normal routine MRI, if DAI is strongly suspected or if evidence of DAI is sought long after trauma, an MRI at 3T would be more appropriate (Guo et al., 2013b).

One study attempted to relate traumatic hemorrhage burden to injury severity using GRE (Haacke et al., 2010), and found that with sufficient resolution, major veins and related hemorrhage in the brain could be visualized. Scheid et al. (2003) scanned 66 patients at the chronic stage after TBI using a 3T magnet with a T2*-weighted GRE sequence. Traumatic microbleeds were revealed in 46 (69.7%) patients by T2*-weighted GRE imaging. Compared with T1-weighted GRE imaging, T2*-weighted imaging showed significantly

more traumatic microbleeds ($P = 0.000$). Although there was a significant correlation between the total number of callosal traumatic microbleeds and GCS scores ($P = 0.000$), no correlation was found with extended GOS scores. High field strength T2*-weighted GRE imaging is a useful tool for the evaluation of DAI during the chronic stage of TBI. Gao et al. (2013) showed that brain lesions related to DAI are predominantly hemorrhagic and they concluded that the T2*-weighted GRE imaging is good for initial diagnosis, but not for long-term prognosis. They suggested the use of other sequences, such as susceptibility tensor imaging, diffusion tensor imaging, or MR spectroscopy, for long-term outcome prediction (Li et al., 2013a; Wei et al., 2013). However, Scheid et al. (2003) revealed that TMB load is not a sufficient parameter for assessing the severity of DAI or for making a prognosis of functional outcome (Scheid et al., 2003). See **Figure 1**.

SWI and SWI with Mapping (SWIM)

SWI is even more sensitive to hemosiderin deposition and is superior to conventional MRI for detecting microbleeds in the brain after trauma. The SWI method was originally used to enhance the visibility of small veins. Each final SWI image is made by collapsing several adjacent slices, and usually shows the contiguity of vessels. Occasionally, several contiguous images can be reviewed to follow a vessel. Detection of CMBs has improved rapidly over recent years with the advent of SWI and it has become a very promising method for detecting TBI (Kou et al., 2010). In fact, it has been used for some time as a means to enhance venous signal using high-pass filtered phase images (Zhao et al., 2013; Zhu et al., 2013i). SWI is a gradient-echo MRI technique, and post processing software is designed to detect small changes in local magnetic susceptibility in the brain tissue. This allows sensitive detection of paramagnetic effects using information from the phase image (Warner et al., 1988c). It takes advantage of the fact that tissue types are differentially susceptible to magnetism to enhance their intrinsic contrasts. Many pathological states can be better visualized by SWI compared with other MRI techniques, including neuro-vasculature abnormalities, calcification, iron deposits, hemorrhage, and change in oxygenation levels that result from altered blood flow or pathological processes. SWI has the potential to improve detection of traumatic micro-hemorrhagic lesions that are invisible or inconspicuous on conventional MRI, to categorize clinical injury severity, and to predict long-term neurocognitive outcomes. The technique is easy to implement and may prove helpful in the evaluation of venous diseases, even when they affect veins with diameters smaller than 0.5 mm (Warner et al., 1988b). SWI is a more sensitive means to detect hemorrhagic DAI than is conventional T2*-weighted gradient-echo sequences. More accurate and objective assessment of injury can be obtained in the early post trauma phase. In this phase, prognostic information regarding duration of coma is also useful. SWI has been noted to be better than other techniques not only for detecting small hemorrhages in the absence of other abnormal findings, but also for documenting the presence of brain injury, thereby increasing the quality of patient management. The number and volume of lesions as identified by SWI show a negative correlation with patients' clinical outcomes (Zhu and Wang, 2013) and neuropsychological functions (Zhu et al., 2013d; Chen et al., 2014). See **Figure 2**.

As reported by conventional CT and MRI studies, traumatic hemorrhages are usually found in cortical gray matter, subcortical white matter, major white matter tracts, and the ventricles (Guo et al., 2013a). In addition to these locations, SWI has shown micro-hemorrhagic lesions at gray matter/white matter junctions, vessel junctions, and more importantly, in veins. These days, with increased use of GRE T2*-weighted MRI sequences and SWI-MRI sequences, detection of CMBs and other forms of intracranial hemorrhages have significantly increased (Li et al., 2013b). In an SWI-MRI and T2*-weighted MRI-imaging study conducted in 15 individuals, it was found that SWI detected a mean of 76 ± 52 (total 1,132) hypointense spotty lesions, whereas, T2-weighted image detected only 21 ± 19 (total 316) lesions. Thus, SWI is more sensitive than conventional T2-weighted imaging in detecting small hemorrhages associated with DAI (Liu et al., 2013a). Tong et al. (2003) performed a retrospective study in seven children and adolescents with TBI who were admitted to an intensive care unit with presumed DAI. They compared the effectiveness of SWI and conventional GRE sequences in detecting small hemorrhagic lesions. MRI (1.5T) was taken within 11 days of injury. Results showed that compared with GRE images there was 3- to 6-fold increase in lesion detection and 2-fold increase in the total apparent volume of hemorrhagic DAI lesions when using SWI images. Lesion detection was relatively greater in the brainstem, cerebellum, and corpus callosum than in frontal, parietal, temporal, and occipital gray/white matter junctions. Another study conducted in 141 individuals using both GRE and SWI showed that prevalence of microbleeds was 23% on GRE images and 40% on SWI images. Irrespective of CMB locations, 284 CMBs were detected on SWI sequences, whereas only 219 CMBs were detected on GRE sequences (Zeng et al., 2013). SWI sequences also appeared to detect much smaller hemorrhagic lesions, the majority of them being about 10 mm^2, while those detected by GRE sequences were 11–20 mm^2 (Hosking et al., 1989). A report suggests that quantitative imaging of micro-hemorrhages as a surrogate marker of brain injury can be used to rank injury severity (Zhou et al., 2013). Babikian et al. (2005) have also demonstrated the prognostic use of regional SWI-lesion quantification with regard to neuropsychological outcomes at 6 months to 1 year.

Indeed, SWI does show promise in predicting long-term outcome. Sigmund et al. (2007) evaluated 40 children and adolescents (mean age 12 years, scanned 7 ± 4 days after injury) with presumed DAI and tried to determine which MRI method was more effective in predicting 6–12 months outcomes as classified by the Pediatric Cerebral Performance Category Scale score. Results showed that SWI-MRI sequences were better for assessing the injury severity and de-

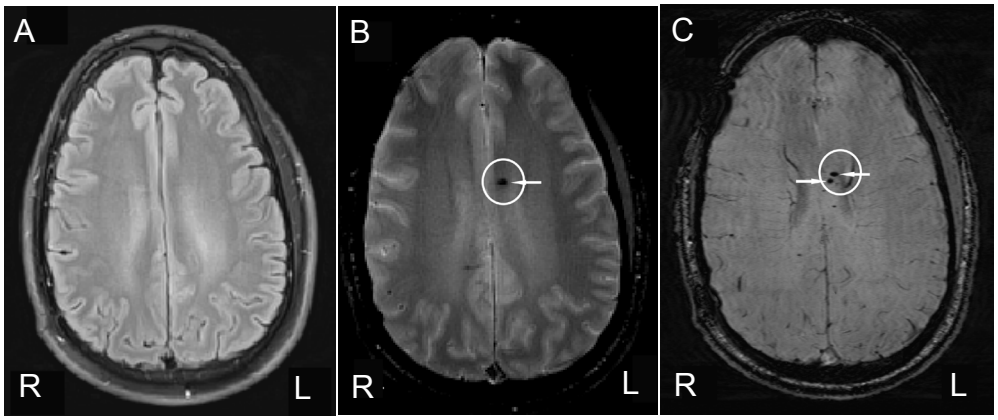

(A) T2 flair imaging shows no abnormalities. (B) GRE imaging shows one periventricular lesion (white arrow in white circle). (C) SWI imaging shows two lesions at the same location (white arrows in white circle). The SWI sequence shows more lesions than the other sequences do. R: Right; L: left.

Figure 1 Image of the brain of a male patient (42 years old) taken with a 3T (Siemens, Magnetom Trio, Germany) magnetic resonance system 3 months after traumatic brain injury.

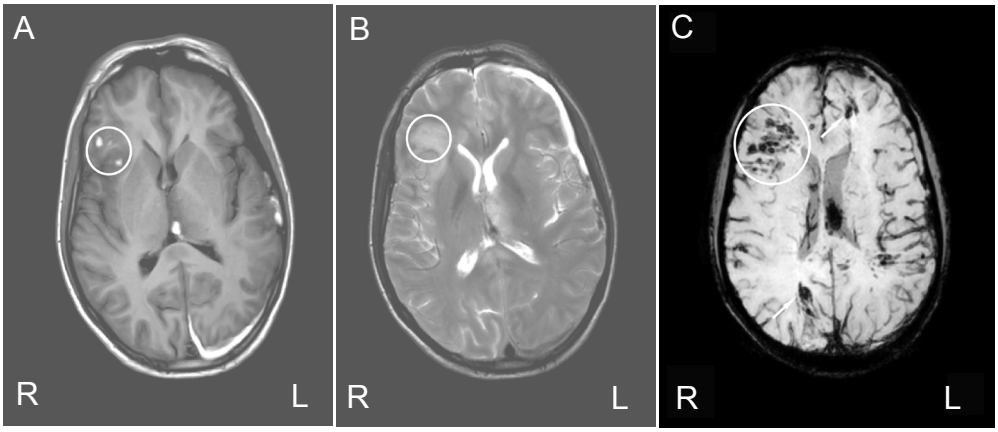

(A) A T1-weighted image shows high intensity lesions in the temporal lobe and left thalamus (white circle). (B) T2-weighted image shows low intensity hemorrhage and edema at the same location (white circle). (C) SWI shows more lesions at the same location and also other lesions in the left frontal lobe and right occipital lobe (white circle and white arrows). R: Right; L: left.

Figure 2 Image of the brain of a male patient (23 years old) taken with a 3T (Philips, Hoffman-LaRoche, Mijdrecht, the Netherlands) magnetic resonance system 1 day after traumatic brain injury.

tecting the lesions that affected the outcomes. Chastain et al. (2009) suggest that GRE-imaging, in the form of SWI, which is extremely sensitive to small changes in T2* associated with hemorrhage, is capable of detecting micro-hemorrhages associated with DAI and can help to rank the degree of brain injury and predictions of outcome.

The method by which MRI images are obtained after post-processing using an inverse procedure to generate susceptibility maps of the veins is called SWIM (Haacke et al., 2010). Regardless of the size and orientation of the veins, SWIM can successfully create venograms of the brain and make imaging process easy (Ding et al., 2013). The images show a new form of MR venography and can serve as a quantitative means to distinguish potential oxygen-saturation abnormalities in SWI data (Labaceno Gainza et al., 1989). The measurement of magnetic susceptibility offers an entirely new form of contrast in magnetic resonance imaging and provides a new quantitative measure of extravasated blood (Lin et al., 2013; Zhu et al., 2013e; Zhu et al., 2013h). A study reported that the total susceptibility of a CMB measured using quantitative susceptibility mapping (QSM) is a physical property that is independent of echo time (Lu et al., 2013). See **Figure 3**.

Diffusion tensor imaging (DTI)

Magnetic resonance DTI is used to evaluate the structural and physiological state of biological tissue by detecting water molecules based on the microscopic random motion law, and enables measurement of the anisotropic diffusion of water in tissue. By determining the dominant direction of water-molecule diffusion in the white matter, it not only helps to accurately distinguish white matter from gray matter, but also helps follow the direction of white matter fiber tracts, thus allowing a good imaging result. DTI can be used to identify white matter fiber-tract lesions caused by pressure-shift infiltration and destruction, and is recognized today as the most promising non-invasive method to observe white matter fiber bundles with complete spatial orientation. The extent of white matter fractional anisotropy (FA) and apparent diffusion coefficient (ADC) indirectly reflect the degree of myelination and integrity of the fiber bundle (Warner et al., 2010; Zhu et al., 2013g). In mild head injury, neurofilaments can be damaged, altering the transport processes along the axon and local cellular trans-

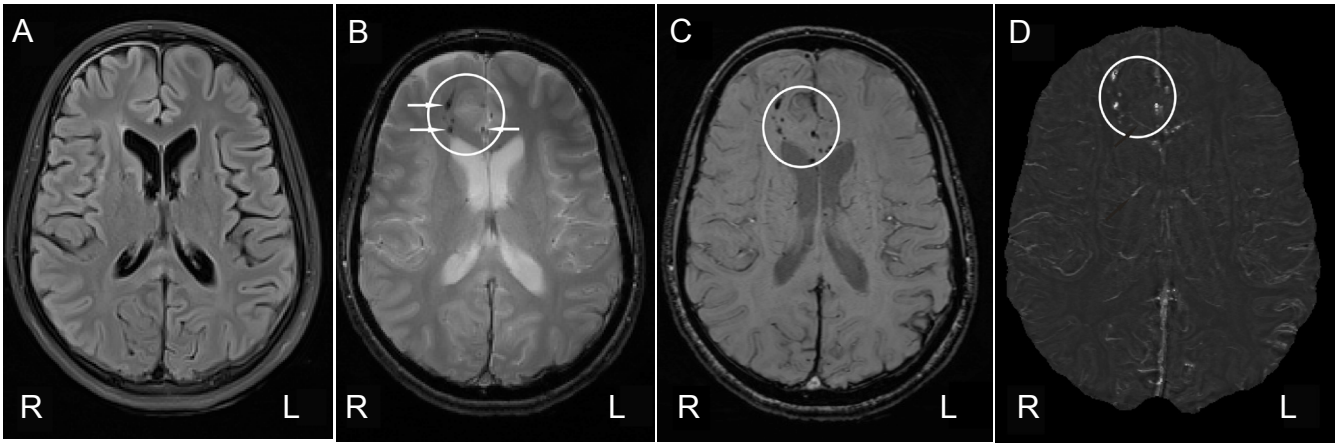

Figure 3 Image of the brain of a female patient (38 years old) on a 3T (Simens) magnetic resonance system 2 months after traumatic brain injury.
(A) T2 flair imaging shows no abnormalities. (B) Gradient Echo imaging shows three lesions in the right frontal lobe (white arrows in white circle). (C) Susceptibility-weighted imaging shows more low intensity lesions at the same location and also in the corpus callosum (white circle). (D) Susceptibility-weighted imaging mapping shows high intensity lesions (white circle) and deep veins (black arrow). R: Right; L: left.

port processes. This leads to axonal swelling and increased permeability of the membrane resulting in an increase in the diffusion coefficient perpendicular to the axonal plane and a decrease in the one parallel to it. Conventional CT and MRI cannot display these changes, but DTI can be used to quantitatively analyze the change in FA values and ADC values in the region of interest (ROI), thereby effectively predicting the occurrence and extent of neurocognitive function impairment after concussion. Because conventional CT and MRI often show no abnormalities, a DTI scan is a better indicator for initial evaluations of patients in head trauma clinics who complain of significant headache, dizziness, vertigo, vomiting, and lethargy. If the FA signal is normal, symptoms will usually disappear, but if FA signals show abnormalities, neurotrophic management and protection should be considered. Thus, DTI is of practical use for clinical treatment (Shenton et al., 2012).

Krishna et al. (2012) found that in cases of mild head injury, significantly lower FA signals and elevated ADC values indicate a poor prognosis that includes axonal swelling as an early manifestation of axonal injury. Aoki et al. (2012) conducted a study in 13 patients with mild TBI, and found that DTI can detect FA values for different regions and different fiber bundles. Compared with the controls, FA values were significantly lower, white matter fiber-bundles were reduced, and interruptions were found in the corpus callosum. Metting et al. (2013) conducted a DTI study on 18 subjects with mild TBI and found that compared with the normal control group, bilateral frontal white-matter FA values were significantly lower and in the temporal top diffusivity was (mean diffusivity, MD) was higher. Cerebral hemorrhage volume is closely related to FA values in regions with large white-matter fiber bundles, such as the corpus callosum, internal capsule, inferior frontal occipital fasciculus, corticospinal tract, and the upper and lower longitudinal fasciculus.

Conclusions and future directions

CMBs can be viewed as markers of strain that exceed the elastic limits of vessel walls. As such, they are dual biomarkers, both of damage to tissue and of the forces that caused the damage. The latter has implications for informing and improving models of the brain's response to linear and angular forces, where the goal is to improve the design of protective equipment to reduce or eliminate injury.

MRI methodology along with its application in the medical field has undergone dramatic advances in the last 30 years. Recently developed MRI methods are excellent diagnostic tools for detecting and localizing numerous pathologic and pathophysiologic changes resulting from TBI. SWI is one of the most sensitive imaging methods for detecting CMBs and for evaluating the progression of TBI. SWI is three to six times more sensitive to blood products than the clinical standard GRE T2*-weighted sequence, depending on the field strength, reconstruction techniques, and echo times that are used. Additionally, it is particularly well suited to investigating TBI, where small hemorrhages are an indirect marker of axonal injury and vascular rupture (Wang et al., 2014b).The ability to detect microhemorrhagic lesions in TBI has contributed to improved categorization of injuries and prediction of functional outcomes at 6–12 months. At the same time, manual rating of CMBs is less reliable and more time consuming. To overcome this problem, Seghier et al. (2011) developed a technique called microbleed detection using automated segmentation (MIDAS). This post-processing method can identify microbleeds on standard MR data sets with results that are comparable to a validated visual rating system, thus making it a useful screening tool for multiple lobar microbleeds. In another way, relatively new MRI techniques such as SWI, DTI, and magnetic resonance spectrum imaging are very useful for making precise diagnoses and giving reasonable prognoses regarding the clinical outcomes of cases with TBI. These techniques help to broaden our understanding of the brain by revealing the multifaceted nature of injuries. The findings revealed by these sophisticated MRI techniques can serve as biomarkers of different TBI

pathologies, aiding clinicians in classifying patients into different treatment groups, and thus improving the outcomes of specific therapeutic procedures.

In the future, CMBs as well as damage to major veins and other substances in the brain will be perfectly ranked based on their magnetic susceptibilities as determined by QSM longitudinal studies using these MRI techniques. The lesions will be categorized from acute to chronic stage in correlation with neurocognitive assessments. SWIM will continue to improve as a means to visualize veins and quantify oxygen saturation (Haacke et al., 2010). Through the pertinent application of these modern sophisticated MRI methods, dynamic pictures of brain injury can be revealed, and at the same time, the optimal imaging technique can be used at different times for effective outcome prediction.

Author contributions: *Liu J conceived the study and drafted the paper. Kou ZF revised the paper. Tian YQ finalized the article. All authors approved the final version of this paper.*
Conflicts of interest: *None declared.*

References

Aoki Y, Inokuchi R, Gunshin M, Yahagi N, Suwa H (2012) Diffusion tensor imaging studies of mild traumatic brain injury: a meta-analysis. J Neurol Neurosurg Psychiatry 83:870-876.

Babikian T, Freier MC, Tong KA, Nickerson JP, Wall CJ, Holshouser BA, Burley T, Riggs ML, Ashwal S (2005) Susceptibility weighted imaging: neuropsychologic outcome and pediatric head injury. Pediatr Neurol 33:184-194.

Cai J, Ma H, Huang F, Zhu D, Bi J, Ke Y, Zhang T (2013) Correlation of bevacizumab-induced hypertension and outcomes of metastatic colorectal cancer patients treated with bevacizumab: a systematic review and meta-analysis. World J Surg Oncol 11:306.

Chastain CA, Oyoyo UE, Zipperman M, Joo E, Ashwal S, Shutter LA, Tong KA (2009) Predicting outcomes of traumatic brain injury by imaging modality and injury distribution. J Neurotrauma 26:1183-1196.

Chen C, He C, Zhu D, Guo R, Zhang F, Pan S (2013a) Generation of a flat optical frequency comb based on a cascaded polarization modulator and phase modulator. Opt Lett 38:3137-3139.

Chen CT, Li Y, Zhang J, Wang Y, Ling HW, Chen KM, Gao PJ, Zhu DL (2014) Association between ambulatory systolic blood pressure during the day and asymptomatic intracranial arterial stenosis. Hypertension 63:61-67.

Chen J, Zhou C, Wu B, Wang Y, Li Q, Wei Y, Yang D, Mu J, Zhu D, Zou D, Xie P (2013) Left versus right repetitive transcranial magnetic stimulation in treating major depression: a meta-analysis of randomised controlled trials. Psychiatry Res 210:1260-1264.

Costello MG, Zhu D, Salinas E, Stanford TR (2013) Perceptual modulation of motor--but not visual--responses in the frontal eye field during an urgent-decision task. J Neurosci 33:16394-16408.

Ding Y, Wang J, Fan Z, Wei D, Shi R, Luo Q, Zhu D, Wei X (2013) Signal and depth enhancement for in vivo flow cytometer measurement of ear skin by optical clearing agents. Biomed Opt Express 4:2518-2526.

Finkelstein EA, Corso PS, Miller TR (2006) Incidence and economic burden of injuries in the United States. Oxford: Oxford University Press.

Fu Y, He Q, Zhu D, Wang Y, Gao Y, Cao H, Cheng J (2013) A BODIPY dye as a reactive chromophoric/fluorogenic probe for selective and quick detection of vapors of secondary amines. Chem Commun (Camb) 49:11266-11268.

Gao J, Gong H, Huang X, Fang J, Zhu D, Fan Y (2013) Relationship between microstructure, material distribution, and mechanical properties of sheep tibia during fracture healing process. Int J Med Sci 10:1560-1569.

Gao X, Jia R, Wang M, Zhu D, Chen S, Lin M, Yin Z, Wang Y, Chen X, Cheng A (2014) Construction and identification of a cDNA library for use in the yeast two-hybrid system from duck embryonic fibroblast cells post-infected with duck enteritis virus. Mol Biol Rep 41:467-475.

Glenski JA, Warner MA, Dawson B, Kaufman B (1984) Postoperative use of epidurally administered morphine in children and adolescents. Mayo Clin Proc 59:530-533.

Guo Q, Zhuo C, Xu Y, Huang W, Wang C, Zhang S, Huang J, Hu F, Zhu D, Yang F, Wang M (2014) Genetic diversity of fluoroquinolone-non-susceptible Streptococcus pneumoniae clinical isolates and the first identification of serotype 20B in China. Eur J Clin Microbiol Infect Dis 33:465-470.

Guo Z, Hu RJ, Zhu DM, Zhu ZQ, Zhang HB, Wang W (2013b) Usefulness of deep hypothermic circulatory arrest and regional cerebral perfusion in children. Ther Hypothermia Temp Manag 3:126-131.

Haacke EM, Tang J, Neelavalli J, Cheng YC (2010) Susceptibility mapping as a means to visualize veins and quantify oxygen saturation. J Magn Reson Imaging 32:663-676.

Hosking MP, Warner MA, Lobdell CM, Offord KP, Melton LJ, 3rd (1989) Outcomes of surgery in patients 90 years of age and older. JAMA 261:1909-1915.

Hou W, Guo J, Xu X, Wang Z, Zhang D, Wan H, Song Y, Zhu D, Xu Y (2013) Syntheses, structures and properties of two 2-D layered hybrid organic-inorganic materials based on different V4O12 building units. Dalton Trans 43:865-871.

Brain imaging and behavior.Jiang X, Zhu D, Li K, Zhang T, Shen D, Guo L, Liu T (2013). Predictive models of resting state networks for assessment of altered functional connectivity in MCI. Med Image Comput Comput Assist Interv 16:674-681.

Ju MJ, Tu GW, Han Y, He HY, He YZ, Mao HL, Wu ZG, Yin YQ, Luo JF, Zhu DM, Luo Z, Xue ZG (2013) Effect of admission time on mortality in an intensive care unit in Mainland China: a propensity score matching analysis. Crit Care 17:R230.

Kang F, Zhu D (2013) Abiotic reduction of 1,3-dinitrobenzene by aqueous dissolved extracellular polymeric substances produced by microorganisms. J Environ Qual 42:1441-1448.

Kou Z, Wu Z, Tong KA, Holshouser B, Benson RR, Hu J, Haacke EM (2010) The role of advanced MR imaging findings as biomarkers of traumatic brain injury. J Head Trauma Rehabil 25:267-282.

Krishna R, Grinn M, Giordano N, Thirunavukkarasu M, Tadi P, Das S (2012) Diagnostic confirmation of mild traumatic brain injury by diffusion tensor imaging: a case report. J Med Case Rep 6:66.

Labaceno Gainza D, Warner Magnus NM, Jarvis Sánchez D (1989) Congenital cardiovascular malformations. January to July 1987. Rev Cubana Enferm 5:51-55.

Li P, Pan F, Hao Y, Feng W, Song H, Zhu D (2013a) SGK1 is regulated by metabolic-related factors in 3T3-L1 adipocytes and overexpressed in the adipose tissue of subjects with obesity and diabetes. Diabetes Res Clin Pract 102:35-42.

Li Q, Wei L, Xie Y, Zhang K, Liu L, Zhu D, Jiao J, Chen Y, Yan S, Liu G, Mei L (2013) ZnO nanoneedle/H2O solid-liquid heterojunction-based self-powered ultraviolet detector. Nanoscale Res Lett8:415.

Lin S, Li T, Zhu D, Ma C, Wang Y, He L, Zhu C, Xing Q (2013) The association between GAD1 gene polymorphisms and cerebral palsy in Chinese infants. Tsitol Genet 47:22-27.

Liu D, Wang B, Kang Y, Zhu D, Yin WH (2013a) The study of pro-B-type natriuretic peptide in the evaluation of the cardiac function in patients with severe sepsis. Zhonghua Wei Zhong Bing Ji Jiu Yi Xue 25:584-588.

Liu Q, Jia R, Wang M, Huang J, Zhu D, Chen S, Yin Z, Wang Y, Chen X, Cheng A (2013b) Cloning, expression and purification of duck hepatitis B virus (DHBV) core protein and its use in the development of an indirect ELISA for serologic detection of DHBV infection. Arch Virol.

Lu Q, Ren S, Lu M, Zhang Y, Zhu D, Zhang X, Li T (2013) Computational prediction of associations between long non-coding RNAs and proteins. BMC genomics 14:651.

Metting Z, Cerliani L, Rodiger LA, van der Naalt J (2013) Pathophysiological concepts in mild traumatic brain injury: diffusion tensor imaging related to acute perfusion CT imaging. PLoS One 8:e64461.

Mori Y, Murakami M, Arima Y, Zhu D, Terayama Y, Komai Y, Nakatsuji Y, Kamimura D, Yoshioka Y (2014) Early pathological alterations of lower lumbar cords detected by ultrahigh-field MRI in a mouse multiple sclerosis model. Int Immunol 26:93-101.

Scheid R, Preul C, Gruber O, Wiggins C, von Cramon DY (2003) Diffuse axonal injury associated with chronic traumatic brain injury: evidence from T2*-weighted gradient-echo imaging at 3 T. AJNR Am J Neuroradiol 24:1049-1056.

Seghier ML, Kolanko MA, Leff AP, Jager HR, Gregoire SM, Werring DJ (2011) Microbleed detection using automated segmentation (MIDAS): a new method applicable to standard clinical MR images. PLoS One 6:e17547.

Shenton ME, Hamoda HM, Schneiderman JS, Bouix S, Pasternak O, Rathi Y, Vu MA, Purohit MP, Helmer K, Koerte I, Lin AP, Westin CF, Kikinis R, Kubicki M, Stern RA, Zafonte R (2012) A review of magnetic resonance imaging and diffusion tensor imaging findings in mild traumatic brain injury. Brain Imaging Behav 6:137-192.

Shi L, Fu Y, He C, Zhu D, Gao Y, Wang Y, He Q, Cao H, Cheng J (2013a) A mild and catalyst-free conversion of solid phase benzylidenemalononitrile/benzylidenemalonate to N-benzylidene-amine and its application for fluorescence detection of primary alkyl amine vapor. Chem Commun (Camb) 50:872-874.

Shi R, Chen ZY, Zhu DW, Li C, Shan Y, Xu G, Lin SX (2013b) Crystal structures of human muscle fructose-1,6-bisphosphatase: novel quaternary states, enhanced AMP affinity, and allosteric signal transmission pathway. PLoS One 8:e71242.

Shimizu A, Kawana-Tachikawa A, Yamagata A, Han C, Zhu D, Sato Y, Nakamura H, Koibuchi T, Carlson J, Martin E, Brumme CJ, Shi Y, Gao GF, Brumme ZL, Fukai S, Iwamoto A (2013) Structure of TCR and antigen complexes at an immunodominant CTL epitope in HIV-1 infection. Sci Rep 3:3097.

Sigmund GA, Tong KA, Nickerson JP, Wall CJ, Oyoyo U, Ashwal S (2007) Multimodality comparison of neuroimaging in pediatric traumatic brain injury. Pediatr Neurol 36:217-226.

Song B, Zhang ZZ, Zhong JC, Yu XY, Oudit GY, Jin HY, Lu L, Xu YL, Kassiri Z, Shen WF, Gao PJ, Zhu DL (2013) Loss of angiotensin-converting enzyme 2 exacerbates myocardial injury via activation of the CTGF-fractalkine signaling pathway. Circ J 77:2997-3006.

Sun CY, Wang XL, Zhang X, Qin C, Li P, Su ZM, Zhu DX, Shan GG, Shao KZ, Wu H, Li J (2013a) Efficient and tunable white-light emission of metal-organic frameworks by iridium-complex encapsulation. Nat Commun 4:2717.

Sun M, Zhu D, Ji W, Jing P, Wang X, Xiang W, Zhao J (2013) Exploring the effect of band alignment and surface states on photoinduced electron transfer from CuInS2/CdS core/shell quantum dots to TiO2 electrodes. ACS Appl Mater Interfaces 5:12681-12688.

Tao RR, Wang H, Hong LJ, Huang JY, Lu YM, Liao MH, Ye WF, Lu NN, Zhu DY, Huang Q, Fukunaga K, Lou YJ, Shoji I, Wilcox CS, Lai EY, Han F (2014) Nitrosative stress induces peroxiredoxin 1 ubiquitination during ischemic insult via E6AP activation in endothelial cells both in vitro and in vivo. Antioxid Redox Signal[Epub ahead of print].

Tchekmedyian A, Amos CI, Bale SJ, Zhu D, Arold S, Berrueta J, Nabon N, McGarrity T (2013) Findings from the peutz-jeghers syndrome registry of uruguay. PLoS One 8:e79639.

Tie G, Dai Y, Guan C, Zhu D, Song B (2013) Error analysis of compensation cutting technique for wavefront error of KH2PO4 crystal. Appl Opt 52:6645-6651.

Tong KA, Ashwal S, Holshouser BA, Shutter LA, Herigault G, Haacke EM, Kido DK (2003) Hemorrhagic shearing lesions in children and adolescents with posttraumatic diffuse axonal injury: improved detection and initial results. Radiology 227:332-339.

Wang H, Zhao T, Xu F, Li Y, Wu M, Zhu D, Cong X, Liu Y (2014) How important is differentiation in the therapeutic effect of mesenchymal stromal cells in liver disease? Cytotherapy 16:309-318.

Wang L, Ji H, Li M, Zhou J, Bai W, Zhong Z, Li N, Zhu D, Zhang Z, Liu Y, Wu M (2013) Intrathecal administration of autologous CD34 positive cells in patients with past cerebral infarction: A safety study. ISRN Neurol 2013:128591.

Wang XY, Wang P, Qi YP, Zhou CP, Yang LT, Liao XY, Wang LQ, Zhu DH, Chen LS (2014a) Effects of granulation on organic acid metabolism and its relation to mineral elements in Citrus grandis juice sacs. Food Chem 145:984-990.

Wang Y, Feng Y, Jia Y, Wang W, Xie Y, Guan Y, Zhong S, Zhu D, Huang L (2014b) Auditory M50 and M100 sensory gating deficits in bipolar disorder: A MEG study. J Affect Disord 152-154:131-138.

Wang YP, Li ZP, Bai Q, Chen SM, Wang FF, Zhu D, Ren C, Guo LJ, Gao W (2013c) Current status of morning blood pressure control and medication of hypertensive patients in Beijing. Zhonghua Xin Xue Guan Bing Za Zhi 41:587-588.

Warner DO, Warner MA, Divertie MB (1988a) Open lung biopsy in patients with diffuse pulmonary infiltrates and acute respiratory failure. Am Rev Respir Dis 137:90-94.

Warner MA, Warner ME, Buck CF, Segura JW (1988b) Clinical efficacy of high frequency jet ventilation during extracorporeal shock wave lithotripsy of renal and ureteral calculi: a comparison with conventional mechanical ventilation. J Urol 139:486-487.

Warner MA, Hosking MP, Lobdell CM, Offord KP, Melton LJ, 3rd (1988c) Surgical procedures among those greater than or equal to 90 years of age. A population-based study in Olmsted County, Minnesota, 1975-1985. Ann Surg 207:380-386.

Warner MA, Marquez de la Plata C, Spence J, Wang JY, Harper C, Moore C, Devous M, Diaz-Arrastia R (2010) Assessing spatial relationships between axonal integrity, regional brain volumes, and neuropsychological outcomes after traumatic axonal injury. J Neurotrauma 27:2121-2130.

Wei L, Zhu D, Zhou J, Zhang J, Zhu K, Du L, Hua Q (2014) Revealing in vivo glucose utilization of Gluconobacter oxydans 621H Δmgdh strain by mutagenesis. Microbiol Res 169:469-475.

Wu X, Wang Z, Zhu D, Zong S, Yang L, Zhong Y, Cui Y (2013) pH and thermo dual-stimuli-responsive drug carrier based on mesoporous silica nanoparticles encapsulated in a copolymer-lipid bilayer. ACS Appl Mater Interfaces 5:10895-10903.

Xiao J, Xing X, Lu J, Weng J, Jia W, Ji L, Shan Z, Liu J, Tian H, Ji Q, Zhu D, Ge J, Chen G, Chen L, Guo X, Zhao Z, Li Q, Zhou Z, Yang Z, Shan G, et al. (2013a) Prevalence and associated factors of microalbuminuria in Chinese individuals without diabetes: cross-sectional study. BMJ Open 3:e003325.

Xiao ZH, Hu J, Zhu D, Shi YK, Zhang EY (2013b) Tricuspid valve obstruction and right heart failure due to a giant right atrial myxoma arising from the superior vena cava. J Cardiothorac Surg 8: 200.

Xu X, Chen C, Lin D, Guo Q, Hu F, Zhu D, Li G, Wang M (2013) The fosfomycin resistance gene fosB3 is located on a transferable, extrachromosomal circular intermediate in clinical Enterococcus faecium isolates. PLoS One 8:e78106.

Yang D, Liu L, Zhu D, Peng H, Su L, Fu YX, Zhang L (2014) A mouse model for HBV immunotolerance and immunotherapy. Cell Mol Immunol11:71-78.

Yin J, Zhu D, Zhang Z, Wang W, Fan J, Men D, Deng J, Wei H, Zhang XE, Cui Z (2013) Imaging of mRNA-protein interactions in live cells using novel mCherry trimolecular fluorescence complementation systems. PLoS One 8:e80851.

Zen K, Guo Y, Bian Z, Lv Z, Zhu D, Ohnishi H, Matozaki T, Liu Y (2013) Inflammation-induced proteolytic processing of the SIRPalpha cytoplasmic ITIM in neutrophils propagates a proinflammatory state. Nature Commun 4:2436.

Zeng Y, Wang Y, Qu N, Zhu D (2013) Fabrication of a high-aspect-ratio sub-micron tool using a cathode coated with stretched-out insulating layers. Rev Sci Instrum 84:095006.

Zhang D, Hou L, Zhu D, Chen W (2014) Synergistic role of different soil components in slow sorption kinetics of polar organic contaminants. Environ Pollut184:123-130

Zhang J, Li X, Li C, Lian Z, Huang X, Zhong G, Zhu D, Li K, Jin C, Hu X, Han J, Guo L, Hu X, Li L, Liu T (2013a) Inferring functional interaction and transition patterns via dynamic bayesian variable partition models. Hum Brain Mappdoi: 10.1002/hbm.22404.

Zhang S, Zhu D, Wan Z, Cao Y (2014b) Utility of point-of-care ultrasound in acute management triage of earthquake injury. Am J Emerg Med 32:92-95.

Zhang ZZ, Shang QH, Jin HY, Song B, Oudit GY, Lu L, Zhou T, Xu YL, Gao PJ, Zhu DL, Penninger JM, Zhong JC (2013b) Cardiac protective effects of irbesartan via the PPAR-gamma signaling pathway in angiotensin-converting enzyme 2-deficient mice. J Transl Med 11:229.

Zhao C, Bi Q, Hu JT, Xia B, Ying QF, Zhu DJ, Zhang SJ, Gu HF, Hong JF, Qiu BS, Chen Y (2013) Effects of statins upon bone mineral density in postmenopausal women with hypercholesterolemia. Zhonghua Yi Xue Za Zhi 93:2309-2311.

Zhong XF, Zhu D, Lu Q, Liu B, Peng YL (2013) Monitoring renal microcirculation perfusion alteration with contrast-enhanced ultrasound during cardiopulmonary bypass. Sichuan Da Xue Xue Bao Yi Xue Ban 44:646-650.

Zhou WJ, Wang RY, Li Y, Chen DR, Chen EZ, Zhu DL, Gao PJ (2013) A randomized controlled study on the effects of bisoprolol and atenolol on sympathetic nervous activity and central aortic pressure in patients with essential hypertension. PLoS One 8:e72102.

Zhu B, Pan S, Zhu D, Yao J (2013a) Wavelength reuse in a bidirectional radio-over-fiber link based on cross-gain and cross-polarization modulation in a semiconductor optical amplifier. Opt Lett 38:3496-3498.

Zhu D, Wang L (2013) An exact algorithm for the zero exemplar breakpoint distance problem. IEEE/ACM Trans Comput Biol Bioinform 10:1469-1477.

Zhu D, Wallis DJ, Humphreys CJ (2013b) Prospects of III-nitride optoelectronics grown on Si. Rep Prog Phys 76:106501.

Zhu D, Tanabe SH, Yang C, Zhang W, Sun J (2013c) Bacterial community composition of South China Sea sediments through pyrosequencing-based analysis of 16S rRNA genes. PLoS One 8:e78501.

Zhu D, Jin L, Wang X, Xu L, Liu T (2014) Combined anticalcification treatment of bovine pericardium with decellularization and hyaluronic acid derivative. Biomed Mater Eng 24:741-749.

Zhu D, Xu Y, Liu Y, Chen X, Zhao Z, Lei P (2013d) Synthesis of 4″-O-desosaminyl clarithromycin derivatives and their anti-bacterial activities. Bioorg Med Chem Lett 23:6274-6279.

Zhu D, Tong Q, Liu W, Tian M, Xie W, Ji L, Shi J (2013e) Angiotensin (1-7) protects against stress-induced gastric lesions in rats. Biochem Pharmacol [Epub ahead of print].

Zhu D, Li K, Terry DP, Puente AN, Wang L, Shen D, Miller LS, Liu T (2013f) Connectome-scale assessments of structural and functional connectivity in MCI. Hum Brain Mapp doi: 10.1002/hbm.22373.

Zhu D, Zhang T, Jiang X, Hu X, Chen H, Yang N, Lv J, Han J, Guo L, Liu T (2013g) Fusing DTI and fMRI data: A survey of methods and applications. Neuroimage pii: S1053-8119(13)01007-0.

Zhu DL, Gao PJ, Liu SW, Jeong MH, Mattheus M, Birgit V (2013h) Efficacy and tolerability of a single-pill combination of telmisartan/hydrochlorothiazide 80/25 mg in Chinese and Korean patients with moderate to severe hypertension: a subgroup analysis of a randomized, double-blind, active-controlled trial. Chin Med J (Engl) 126:4072-4077.

Zhu da Q, Norman IJ, While AE (2013i) Nurses' self-efficacy and practices relating to weight management of adult patients: a path analysis. Int J Behav Nutr Phys Act 10:131.

Zhu X, Wang Y, Sun Y, Zheng J, Zhu D (2013j) MiR-155 up-regulation by LMP1 DNA contributes to increased nasopharyngeal carcinoma cell proliferation and migration. Eur Arch Otorhinolaryngol [Epub ahead of print].

Copyedited by Liu HM, Li CH, Song LP, Zhao M